Defense Technical Information Center
Compilation Part Notice

ADP014284

TITLE: Anomalous X-ray Scattering for Determination of Nanostructured Alloy Formation and Site-specific Chemistry of Bragg Peak

DISTRIBUTION: Approved for public release, distribution unlimited

This paper is part of the following report:

TITLE: Materials Research Society Symposium Proceedings Volume 740 Held in Boston, Massachusetts on December 2-6, 2002. Nanomaterials for Structural Applications

To order the complete compilation report, use: ADA417952

The component part is provided here to allow users access to individually authored sections of proceedings, annals, symposia, etc. However, the component should be considered within the context of the overall compilation report and not as a stand-alone technical report.

The following component part numbers comprise the compilation report:
ADP014237 thru ADP014305

Anomalous X-ray Scattering for Determination of Nanostructured Alloy Formation and Site-specific Chemistry of Bragg Peak

G.M. Chow*
Department of Materials Science
National University of Singapore
Kent Ridge, Singapore 119260
Republic of Singapore
Email: mascgm@nus.edu.sg

* Also at Singapore-Massachusetts Institute of Technology Alliance (SMA), Republic of
Singapore

ABSTRACT

The properties of nanostructured films can be tailored by many factors such as
composition, structure, preferred orientation, microstructure, interphase interface and grain
boundaries. Compositional control of magnetic properties of recording media depends on the
miscibility of constituent elements. However, for nanostructured materials with a large surface-
to-volume ratio of atoms, the miscibility at the nanoscale may not necessarily follow the
prediction of conventional phase diagram that does not consider the effects of surface and
interface. This limitation further complicates the prediction of phase separation at grain
boundaries and interphase interface. Using anomalous x-ray scattering, the alloying and
composition of a specific long range order of textured nanostructured films has been
investigated. Such information may not be readily available from conventional characterization
techniques.

INTRODUCTION

Nanostructured polycrystalline films have a significant amount of grain boundaries and
interfaces. For many advanced materials such as those used in magnetic applications, careful
control of the grain size, global composition, composition of a specific textured Bragg peak, long
range order (LRO), short range order (SRO) and interphase interfaces, is of essential importance
in order to achieve the desirable properties.

The empirical factors that favor the formation of a binary solid solution can be provided
by the Hume-Rothery's rules [1]. The structural characterization and determination of alloys and
composites by x-ray diffraction (XRD) is also well established [2]. For coarse-grained materials,
the appearance of a single set of diffraction peaks and the disappearance of elemental peaks are
commonly considered as a strong evidence of formation of a solid solution. The variation of
lattice parameter with the composition of a random, substitutional alloy can be qualitatively
followed using the Vergard's law.

When the crystallite size of a material is reduced to below a critical length scale, a nanostructured solid solution cannot be unambiguously differentiated from a nanocomposite using conventional XRD [3]. In a nanocomposite where the two phases have close lattice parameters and x-ray structural coherence, the Bragg peak of one phase has some degree of overlap with that of the other phase. Because of the effect of size broadening and the contribution to diffraction amplitude by structural coherence of the two phases, a single peak will appear for a particular Bragg reflection when the size is below a certain limit. However, this single peak has an average lattice spacing that has no correspondence in real space, and can be easily mistaken as evidence of formation of a solid solution. The critical domain size is mainly determined by the differences in scattering powers and lattice spacings of the constituent elements, and the ability to form coherence interfaces. This consideration is not limited only to XRD, and different scattering powers of different structural techniques result in different critical domain size [3]. Therefore, conventional XRD, commonly established for probing the LRO, should not be used alone to study the structure of nanostructured alloys and composites made of structurally coherent and immiscible materials.

In this paper, an overview of our work on the determination of alloying and composition of a specific Bragg peak of nanostructured magnetic films using synchrotron techniques is presented. The synchrotron techniques, due to the high brightness, flux and resolution, and tunable photon energy, are unique to provide structural and chemical information that is not available from the conventional characterization methods. Using anomalous x-ray scattering, it was shown that nanostructured NiCo films did not necessarily form solid solution as expected from their phase diagram or suggested by the results of conventional XRD [4]. The compositions of constituent elements of the textured Bragg peak of CoCrPt film were also investigated using this method [5]. The limitations of using conventional XRD alone for studying nanostructured alloys are discussed. Advantages of complementary structural investigations using anomalous x-ray scattering (for LRO) and extended x-ray absorption fine structure spectroscopy (for SRO) are presented. The limitations of applying conventional phase diagram to nanostructured materials are also addressed.

RESULTS AND DISCUSSIONS

Ni-Co films [4]

Nickel-cobalt based films find applications in decoration, protection and magnetic applications. Nickel has the fcc structure. Cobalt transforms from the hcp ε phase to the fcc α phase at about 422 °C. The Ni-Co system has complete solid solubility as the (Ni, αCo) phase at temperatures between the solidus and the solvus of the fcc $\leftrightarrow$ hcp transformation temperature. The composition of Ni in the (ε Co) phase is approximately $\leq$ 35 at. % [6]. The lattice constants for fcc Ni and fcc Co are 3.5238 Å and 3.5447 Å, respectively. The K absorption edges for Co and Ni are 7.709 keV and 8.333 keV, respectively.

The Ni_xCo_{100-x} (x = 0, 50, 90 and 100) magnetic films were deposited on Cu substrates using the non-aqueous, electroless polyol method [7]. The magnetic properties of these films can be found elsewhere [7]. Synchrotron specular x-ray scattering, anomalous x-ray scattering (AXS)

and extended x-ray absorption fine structure (EXAFS) spectroscopy were employed to investigate the LRO and SRO of these NiCo films.

Although EXAFS has been widely accepted as a very useful tool to study nanostructured metastable alloys, it is unsuitable for investigating materials consisted of elements (such as Ni and Co) with very close lattice parameters, backscattering amplitudes and phase shifts. The EXAFS results of the Ni edge and Co edge of $Ni_{90}Co_{10}$ and $Ni_{50}Co_{50}$ did not show noticeable difference from the elemental films (Fig. 1). The EXAFS data were therefore inconclusive regarding the mixing of these elements in the films.

Conventional specular XRD results showed these films were polycrystalline and had a single set of fcc diffraction peaks. No elemental separation was detected. Due to the close lattice constants of fcc Ni and fcc Co, the formation of alloy or composite could not be ascertained using XRD. The average crystallite size of Ni_{100}, Co_{100}, $Ni_{90}Co_{10}$ and $Ni_{50}Co_{50}$, as estimated from the (111) line broadening, were 64, 15, 45 and 16 nm, respectively. Only the (111) peaks that gave the strongest signal were used for AXS measurements. Powder diffraction experiments were first performed just below the respective K-edges of Ni and Co to determine the position of the (111) Bragg peak of the films at each photon energy. At the (111) reflection, only a single peak was observed in the $Ni_{50}Co_{50}$ and $Ni_{90}Co_{10}$ films. For AXS measurements, the momentum transfer was fixed to the positions of the (111) reflection, i.e. $q = 3.086 Å^{-1}$, and the scattering intensity was monitored as the x-ray energy was varied through the Ni and Co K-absorption edges, respectively. Good counting statistics was ensured in data collection.

The atomic scattering factor consists of the non-resonant Thomson scattering factor and the resonant anomalous scattering factor. In diffraction measurements, the diffraction intensity is proportional to the square of the atomic factor and shows absorption-like information. If the element in question is related to the specific Bragg peak, then the elemental absorption causes a decrease in the Bragg intensity at its absorption edge. A cusp, due to the interference between the Thomson scattering amplitude and the real part of the anomalous scattering amplitude [8], can be observed in the energy scan of the Bragg peak. This behavior was indeed observed for the Ni_{100} and Co_{100} films.

The AXS measurements of the (111) peaks of $Ni_{50}Co_{50}$ and $Ni_{90}Co_{10}$, around the K-absorption edges of Ni and Co, respectively, are shown in Figs. 2a and 2b. Both Ni and Co were related to this Bragg peak for the $Ni_{50}Co_{50}$ film. Due to their very close lattice parameters, it was not possible to determine if the peak with both elements represented an alloy or a composite. For the $Ni_{90}Co_{10}$ film, only Ni was related to the Bragg peak, whereas the Co absorption was clearly absent. The existence of Co in the $Ni_{90}Co_{10}$ sample was however indeed confirmed by the Co absorption edge in EXAFS and the chemical analysis using energy-dispersive x-ray spectroscopy. Within the detection limit of AXS, Co was not associated with the (111) Bragg peak of this film. Only Ni solely contributed to this Bragg peak. The absence of Co in the (111) Bragg peak of $Ni_{90}Co_{10}$ suggested that Co did not alloy with Ni in this atomic arrangement.

The effects of surface segregation and the correlation with the composition of the LRO need to be addressed. A thermodynamic analysis of a $Ni_{50}Co_{50}$ alloy nanoparticle was carried out to study the influence of size effect on surface compositional segregation[9]. The surface

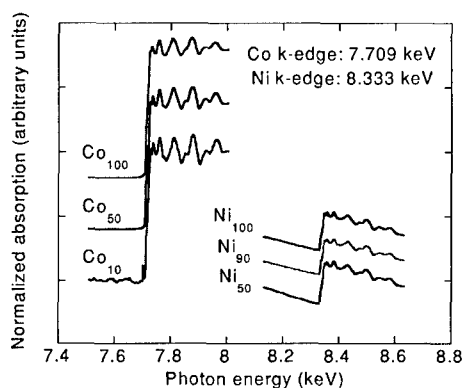Figure 1. Normalized absorption of EXAFS of Ni-Co films, showing both Ni K- and Co K-absorption edges
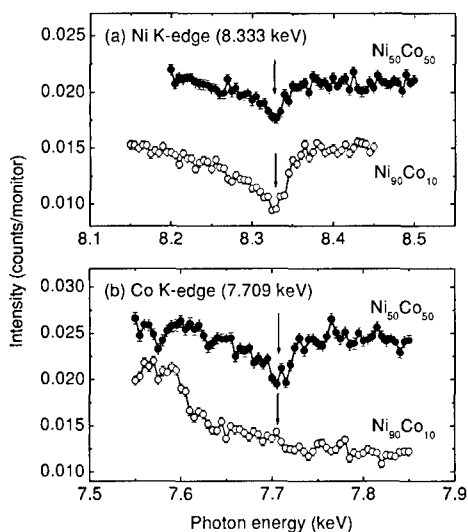

Figure 2. (a) AXS results of $Ni_{50}Co_{50}$ and $Ni_{90}Co_{10}$ films, Ni K-absorption edge. (b) AXS results of $Ni_{50}Co_{50}$ and $Ni_{90}Co_{10}$ films, Co K-absorption edge

compositions of $Ni_{50}Co_{50}$ nanoparticles were calculated based on the regular solution model, that takes into account of the size effect, and compared with that of bulk alloy particles with a larger size. The segregated surface compositions in the alloy nanoparticles (diameter of 10-100 nm) were few times larger than that of the corresponding bulk particles with the particle diameter > 100 nm. Surface segregation would eventually lead to the phase separation beyond a critical size limit for nanostructures.

CoCrPt films [5]

The magnetic properties of sputtered magnetic Co-Cr based films, as longitudinal and perpendicular recording media materials, are controlled by the alloy composition and the degree of phase separation of Co and Cr, the alignment of the columnar structures, the degree of Cr segregation at the grain boundaries and the mosaic of the texture. It is important to achieve a proper crystallographic texture with optimal composition to control the magnetocrystalline anisotropy. The magnetic properties of CoCrPt media films can be optimized by the control of Cr and Pt concentrations that can respectively reduce medium noise and enhance coercivity [10]. The segregation of Cr inhomogeneities in sputtered Co-based films has been considered as Cr segregation at grain boundaries [11], formation of Co_3Cr [12], SRO of Cr [13], formation of Cr oxide at grain boundaries [14], segregated microstructures and two-phase compositional separation [15]. The phase separation occurred by surface diffusion [16] or discontinuous precipitation via grain boundary diffusion [17].

Many characterization techniques, including TEM, x-ray microanalysis, thermo-magnetic analysis, atom-probe field ion microscopy, nuclear magnetic resonance, EXAFS, and STM, have been used to investigate the segregation of Cr. These methods however do not yield direct elemental correlation with the specific LRO of interest. In addition, structural information of compositional segregation cannot be obtained using conventional XRD or TEM, since Co and Cr have similar atomic numbers and scattering factors. It has been commonly but wrongly accepted that a single XRD Bragg peak without detectable elemental separation in these films supports that compositional segregation does not perturb the crystalline order. The conventional phase diagram may not necessarily be applicable in predicting the miscibility or phase separation of nanostructured materials, since it does not take into consideration of the significant contribution of surface and interfaces in these materials. A study was carried out to determine the elemental concentrations of the textured Bragg peak and the averaged local atomic environment of sputtered CoCrPt films using AXS and EXAFS [5].

Both magnetic $Co_{66}Cr_{18}Pt_{16}$ layer (30 nm and 60 nm thick) and Ti underlayer (25 nm thick) were deposited on glass substrates at 250 °C using dc magnetron sputtering. The argon pressure for sputtering Ti and CoCrPt were 3 and 10 mTorr, respectively. Magnetic measurements were performed using VSM. The samples were prepared for structural study without optimizing the magnetic properties.

The x-ray powder scans showed both magnetic layer and Ti underlayer were textured at (002) (Fig. 3). The weak shoulder-peak around $q = 2.959$ Å^{-1} could be assigned to (202) of Ti_2O_3, suggesting the occurrence of Ti underlayer oxidation. The (002) mosaic was obtained

323

from the full-width-half-maximum of the χ rocking curves. The mosaic was large for these films with poor texture. The crystal domain size (estimated from peak broadening) of Ti underlayer was 20 nm and that of 30 nm (60 nm)-thick magnetic film was 30 nm (42 nm), as limited by the respective layer thickness. The VSM hysteresis loops showed these films had perpendicular magnetization orientation. The structure and perpendicular magnetic properties of these films can be found in reference 5. The M_s values were within the reported range for Co-Cr films in this Cr concentration regime [18].

For AXS study, the θ-2θ scan was first performed to determine the position of the CoCrPt (002) reflection (q = 2.984 $\AA^{-1}$) at x-ray energies of 7.509 and 5.789 keV (below the respective K-edges of Co and Cr). There was no detectable phase separation at the (002) reflection (Fig. 3). In AXS, the momentum transfer was fixed to the position of (002) reflection at each photon energy. The scattering intensity was monitored as the x-ray energy was scanned through the Co and Cr K-absorption edges, respectively. The anomalous scattering of Pt was not measured due to the energy limit of the beamline used in this study.
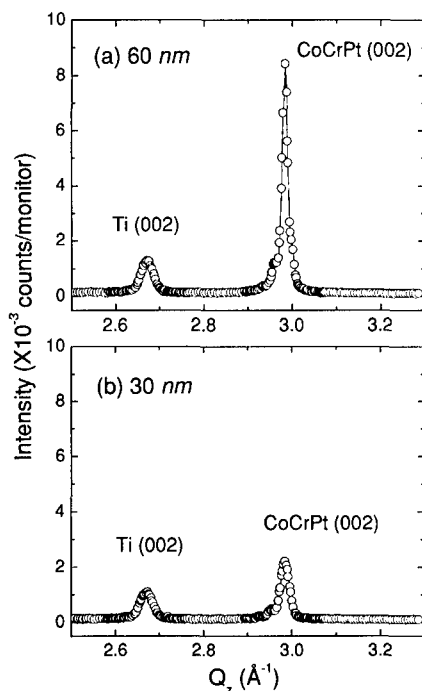

Figure 3. X-ray powder θ-2θ scans of (a) 60 nm film, and (b) 30 nm film

For a qualitative comparison, the measured AXS data was fitted using a film-thickness independent simulation, based on the kinematic approximation of intensity with random mixing of elements. The simulation only considered the concentration of elements in the specific structural order. Figures 4 and 5 show the AXS spectra of the (002) Bragg peak taken in the vicinity of Co and Cr absorption K-edges, respectively. The experimental data was fitted against the simulated spectra using different concentrations. The energy resolution in data collection was estimated as ~7 eV. The Co concentrations in the (002) peak for both films were ~62%, with an estimated uncertainty of ± 5 % (Fig. 4). The Cr concentration in this Bragg peak was ~25 ± 6 % for the 60 nm film, and ~ 22 ± 6 % for the 30 nm film (Fig. 5). Compared to the average global film composition, i.e. $Co_{66}Cr_{18}Pt_{16}$, the concentrations of Co decreased whereas that of Cr increased in the (002) peak.
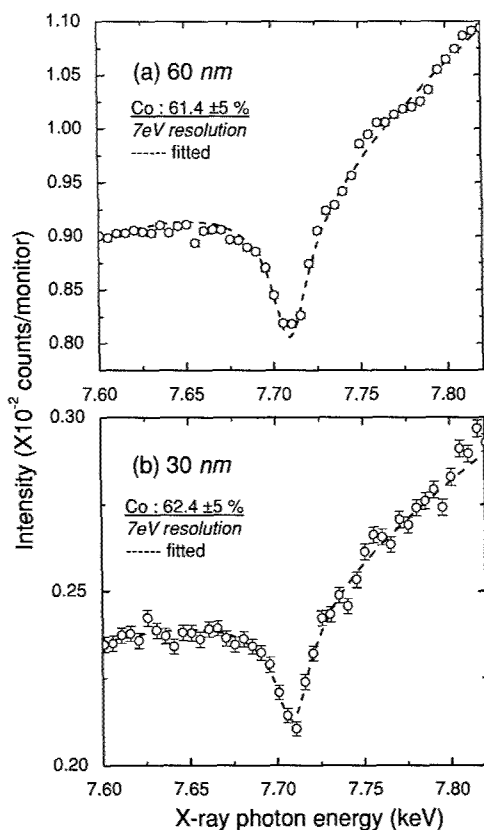

Figure 4. AXS spectra of the (002) peak in the vicinity of Co absorption K-edge. (a) 60 nm film. (b) 30 nm film
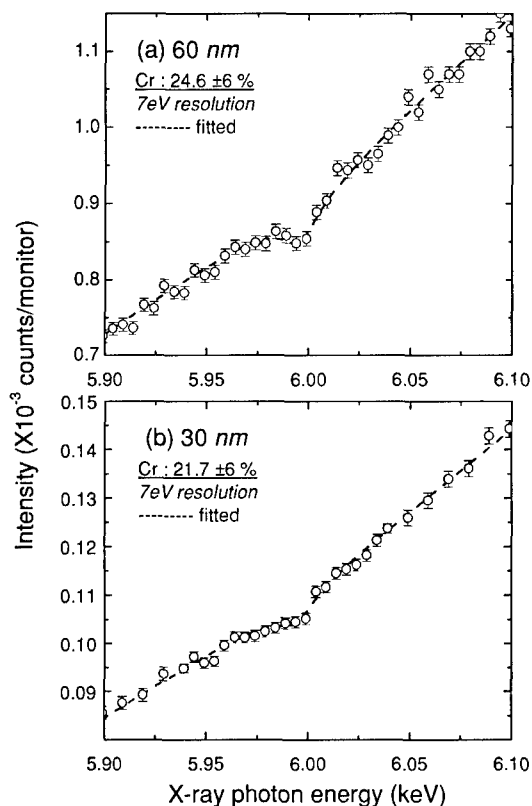
Figure 5. AXS spectra of the (002) peak in the vicinity of Cr absorption K-edge. (a) 60 nm film. (b) 30 nm film

The EXAFS data of Co and Cr were analyzed using a standard WinXAS 97 procedure [19]. The Pt EXAFS was too noisy for useful quantitative analysis as the absorption edge was near the operation limit of the beamline. Figure 6a shows the Fourier Transform amplitude of the Co foil standard, the 30 and 60 nm samples. The coordination number of the first shell of both magnetic films was similar but lower than that of the hcp Co foil standard. This indicated that Co had alloyed with other constituent elements. The Cr EXAFS of both films differed from that of the bcc Cr foil standard (Fig. 6.b).
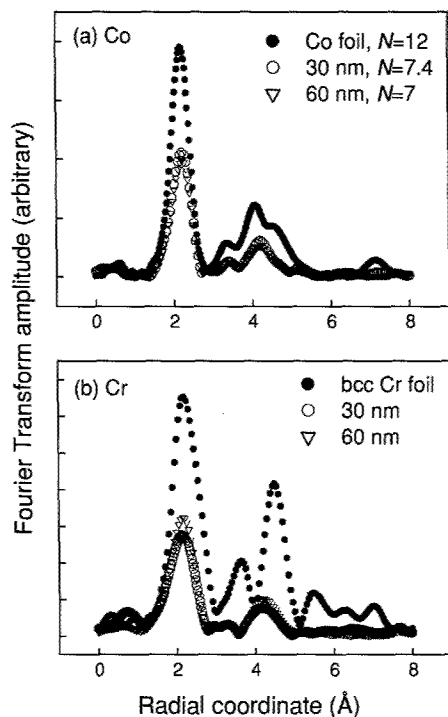
Figure 6. Fourier Transform Amplitude of (a) Co, and (b) Cr. N denotes the coordination number of the first shell

The AXS method only probed the elemental concentrations in the (002) peak, it did not provide the structure information besides this LRO. On the other hand, the EXAFS measurements provided averaged global information of the local atomic environment of the element in question. The AXS results revealed that Co maintained similar concentration in the (002) peak for both films. The EXAFS results showed that both films had similar Co coordination number that was lower than the bulk Co foil. A certain degree of Co alloying with Cr and perhaps Pt had therefore occurred. The dilution of Co by Cr (> 13 %) addition stabilizes perpendicular magnetization and lowers M_s. Compared to the global composition, the higher Cr concentration detected in the (002) peak for both films showed that the crystallinity of Cr was well established.

The observation of a higher Cr content in the textured peak ruled out the common assumption that a significant amount of Cr segregate to the grain boundaries, since grain boundaries are not expected to exhibit any LRO. If the segregation of Cr had resulted in two

crystalline phases, such phases must have the same *d*-spacing as the AXS measurements were fixed at the (002) momentum transfer. The segregation to two crystalline phases with the same *d*-spacing is equivalent to a single phase inhomogeneous alloy. Since Cr did not preferentially segregate to grain boundaries, a resultant higher magnetic exchange coupling [20] and reduced magnetocrystalline anisotropy constant [21] would reduce the coercivity. Since Pt is known to increase the local disorder and thus coercivity by increasing the magnetocrystalline anisotropy [22], the lower coercivity of 60 nm film [5] suggested that less Pt existed in the CoCrPt (002) Bragg peak, compared with that of 30 nm film. This argument is consistent with the observed higher Cr content (Fig. 5) and higher Fourier transform amplitude of Cr edge (Fig. 6b) of the 60 nm thick film. The low sputtering temperature and pressure used in this study could be responsible for inefficient Cr segregation in the grain boundaries [23].

SUMMARY

Conventional x-ray diffraction failed to provide correct information on alloying of materials made of elements with close lattice parameters, even for elements (such as Ni and Co) that are commonly accepted to have miscibility. Using anomalous x-ray scattering, we showed that nanostructured NiCo films did not necessarily form solid solution as expected from their phase diagram or suggested by the results of conventional x-ray diffraction.

The correlation of elemental chemistry with a particular LRO in question cannot be obtained by common conventional characterization techniques. The elemental concentrations of the textured Bragg peak and the averaged local atomic environment of sputtered CoCrPt films were investigated using anomalous x-ray scattering and extended x-ray absorption fine structures. The compositions of constituent elements of the textured peak in these polycrystalline nanostructured films differed from the average film composition. The higher Cr concentration in the textured peak showed that a significant amount of Cr did not segregate to the grain boundaries, as a result of low sputtering temperature and pressure used.

ACKNOWLEDGMENTS

REFERENCES

1. P. Haasen, Physical Metallurgy, 2nd edition, Cambridge University Press, Cambridge, UK, 1986, p. 125.
2. B.D. Cullity, Elements of x-ray diffraction, 2nd edition, Addison-Wesley Publishing Co. Inc., USA, 1978, p. 375.

3. C. Michaelsen, *Phil. Mag. A*, **72**, 813 (1995).
4. G.M. Chow, W.C. Goh, Y.K. Hwu, T.S. Cho, J.H. Je, H.H. Lee, H.C. Kang, D.Y. Noh, C. K. Lin and W. D. Chang, *Appl. Phys. Lett.* **75**,2503 (1999).
5. G.M. Chow, C.J. Sun, E.W. Soo, J.P. Wang, H.H. Lee, D.Y. Noh, T.S. Cho, J.H. Je and Y.K. Hwu, *Appl. Phys. Lett.* **80**,1607 (2002).
6. T. B. Massalski (ed.), Binary alloy phase diagrams, second edition, ASM International, USA, 1990, p. 1214.
7. G.M. Chow, J. Ding, J. Zhang, K.Y. Lee, D. Surani and S.H. Lawrence, *Appl. Phys. Lett.* **74**, 1889 (1999).
8. H. Stragier, J.O. Cross, J.J. Rehr, L.B. Sorensen, C.E. Bouldin and C.E. Woicik, *Phys. Rev. Lett*, **69**, 3064 (1992).
9. R. Jayaganthan and G.M. Chow, *Mater. Sci. Eng. B.* **95**, 116 (2002).
10. M.F. Doerner, T. Yogi, D.S. Parker, S. Lambert, B. Hermsmeier and O.C. Allegranza, *IEEE Trans. Magn.* **29**, 3667 (1993).
11. K. Ouchi and S. Iwasaki, *J. Appl. Phys.* **57**, 4013 (1985).
12. T. Chen, G.B. Charlan and T. Yamashita, *J. Appl. Phys.* **54**, 5103 (1983).
13. W. G. Haines, *J. Appl. Phys.* **55**, 2263 (1984).
14. J.W. Smits, S.B. Luitjens, and F.J.A. den Broeder, *J. Appl. Phys.* **55**, 2260 (1984).
15. D. J. Rogers, Y.Maeda, K. M. Krishnan, *J. Magn. Mag. Mater.* **163**, 393 (1997).
16. K. Hono, K. Yeh, Y. Maeda and T. Sakurai, *Appl. Phys. Lett.* **66**, 1686 (1995).
17. A. Pundt and C. Michaelsen, *Phys. Rev. B.* **56**, 14352 (1997).
18. C.W. Chen, *J. Mater. Sci.* **26**, 1705 (1991).
19. T. Ressler, *J. Physique IV 7*, C2-269 (1997).
20. J. G. Zhu, and H. N. Bertram, *J. Appl. Phys.* **63**, 3248 (1988).
21. I.M. Song, S. Ishio, M. Ishizuka, T. Tsunoda and M. Takahashi, *J. Magn. Magn. Mater.* **119**, 261 (1993).
22. K.M. Kemner, V.G. Harris, W.T. Elam, Y.C. Feng, D.E. Laughlin, J.C. Woicik, and J.C. Lodder, *J. Appl. Phys.* **82**, 2912 (1997).
23. N. Honda, J. Ariake, K. Ouchi and S. Iwasaki, *J. Magn. Magn. Mater.* **155**, 154 (1996).

Synthesis of
Nanostructured Materials I